Probing the YD$_3$ structure by ^{2}H NMR electric-field gradients: A comparison with first-principles calculations

O. J. Żogał

Institute for Low Temperature and Structure Research, Polish Academy of Sciences, P. O. Box 1410, 50-950 Wrocław, Poland

W. Wolf and P. Herzig

Institut für Physikalische Chemie, Universität Wien, Währinger Straße 42, 1090 Vienna, Austria

A. H. Vuorimäki and E. E. Ylinen

Wihuri Physical Laboratory, Department of Physics, University of Turku, 20014 Turku, Finland

P. Vajda

Laboratoire des Solides Irradiés, École Polytechnique, 91128 Palaiseau, Cedex, France

Electric-field gradients (EFG's) in yttrium trideuteride (YD$_{2.98}$) have been determined using deuteron magnetic resonance (DMR) and compared with values for the $P\bar{3}c1$ and $P6_3cm$ structures calculated from first principles. The experimental DMR spectra at low temperatures (180–290 K) could be decomposed into two components with intensity ratio 2:1 in accordance with the expected two groups of deuterium sites, i.e., tetrahedral and octahedral sites in the crystal lattice. Their characteristic quadrupole frequencies, ν_q, and asymmetry parameters, η, have been compared with the theoretical values obtained for the structures with space groups $P\bar{3}c1$ (no. 165) and $P6_3cm$ (no. 185). The agreement between the experimental and calculated results is much better for the latter structure. The spectra at higher temperatures (300–370 K) transform from a two-component configuration into three quadrupolar doublets plus a low-intensity narrow central component. One of the doublets keeps the same parameters as those observed at low temperatures. The two others indicate changes in the tetrahedral site environments. One possible explanation could be a thermally activated quasi-two-dimensional hopping of the D atoms to nearby sites within the ab plane.

INTRODUCTION

Knowledge of the structural arrangement and diffusive motion of hydrogen (deuterium) in the rare-earth trihydrides (trideuterides) is important for gaining a better understanding of their fascinating optical and electrical properties.[1] In particular, the crystallographic structure of YD$_3$ has been a controversial issue. An early neutron powder diffraction study of YD$_3$ (Ref. 2) indicated a structure possessing $P\bar{3}c1$ symmetry, the same as that found for HoD$_3$ (Ref. 3). Subsequently, Udovic *et al.*[4] in their neutron studies indicated that deuterium atoms occupy unusual interstitial positions of a slightly distorted hcp metal instead of the ideal octahedral and tetrahedral sites. More recently, Udovic *et al.*[5,6] concluded that their neutron data could be fitted equally well assuming a structure of $P6_3cm$ rather than $P\bar{3}c1$ symmetry. The authors claim that it cannot easily be distinguished from the $P\bar{3}c1$ structure by neutron powder diffraction measurements, since both structures yield similar powder patterns. Finally (at least, for the moment), Raman effect measurements on YH(D)$_3$ films by Kierey *et al.*[7] showed that the number and the form of the observed phonon modes was not compatible with the $P\bar{3}c1$ structure but pointed rather towards a noncentrosymmetric type such as $P6_3cm$ or $P6_3$.

Apart from experimental work there are many theoretical investigations for YD$_3$. Both the electronic structure and phase stabilities have been the subject of extensive studies.[8–16] Wang and Chou[8,9] and Dekker *et al.*[10] justify the greater stability of the $P\bar{3}c1$ structure for YH$_3$ compared to the alternative fcc structure by total energy calculations based on first principles. However, their results—metallic behavior for this compound—seem to be inconsistent with experimental findings.[1] Next, Kelly *et al.*[11] proposed a lower-symmetry ($P3$) insulating structure. This structure also appeared to be inconsistent with neutron diffraction studies.[4–6] A small energy gap for the $P\bar{3}c1$ structure has been obtained by Ahuja *et al.*[12] and Eder *et al.*[13] The former authors performed total-energy calculations using an all-electron full-potential linear muffin-tin orbital technique while the latter pointed out the importance of electron-correlation effects. Miyake *et al.*,[14] in turn, noted that many-body effects beyond the local-density approximation within an *ab initio* scheme are required to understand the insulating properties of YH$_3$. They made band-structure calculations for the cubic BiF$_3$- and hexagonal LaF$_3$-type structures within the GW approximation. Both calculations produce a band gap of proper size and therefore the authors are inclined to regard the gap as of electronic rather than structural origin. Almost at the same time, van Gelderen *et al.*[15,16] found the desired gap in their GW quasiparticle calculations. Similarly to Miyake *et al.*,[14] their calculations indicate the existence of an energy gap for the hexagonal undistorted LaF$_3$- and distorted HoD$_3$-type structures.

    64 214110-1

In addition to the above-mentioned structural studies, deuteron (^{2}H) NMR can be used to resolve the structural problems faced with YD$_3$ (YH$_3$). Deuterium nuclear-magnetic resonance is sensitive to the electric-field gradient (EFG) at the deuterium atom positions through the quadrupole interaction (QI). The consequence of this interaction, in addition to the dipolar and chemical shift anisotropy, is a specific contribution to the shape of the resonance absorption. While the quadrupole interaction will be zero for a nucleus at a site of cubic symmetry, it is generally nonzero when the nucleus is located at a site with a symmetry lower than cubic. The strength of this interaction depends on the quadrupole moment of the nucleus and the EFG produced by the electrons and other atoms surrounding the nucleus. The EFG can be calculated[17,18] when the crystal structure is available. Then it can be compared with the value obtained from the analysis of the shape of the experimental NMR spectrum.

Three characteristic EFG features in the spectrum at low temperatures (200–330 K) were observed by Balbach *et al.*[19] They were described by them in terms of three different deuterium positions within the HoD$_3$ structure. Two of the features are due to the different octahedral sites and the third one is due to the tetrahedral site. Although they did not calculate EFG values in their paper, the above interpretation seems to be attractive and it is very likely to be correct, except for the observed intensity ratios of the mentioned components. Therefore, the authors do not exclude the interpretation that the $P6_3cm$-type structure would be in better agreement with the NMR data. Earlier perturbed angular correlation (PAC) measurements[20] studying the QI in ^{181}Hf-doped YH$_3$ did not lead to relevant conclusions because of the probable trapping of hydrogen by the rather high concentrations (0.5 at. %) of Hf and its daughter product Ta.

The purpose of this paper is to present our ^{2}H NMR measurements in yttrium trideuteride together with the EFG calculations for the above-mentioned $P\bar{3}c1$- and $P6_3cm$-type structures. The comparison of the EFGs derived from the NMR experiments with those obtained from *ab initio* calculations should indicate the correct structure type. This investigation strongly supports the $P6_3cm$-type structure.

EXPERIMENT

The YD$_{2.98}$ sample was prepared by exposing 99.99 at. % pure yttrium metal obtained from the Ames Laboratory (Ames, Iowa) to deuterium gas. Before deuteriding, the metal was heated to 893 K in vacuum. At 873 K gaseous deuterium generated by heating titanium deuteride was introduced into the reaction vessel. The absorption was performed at a deuterium pressure lower than 1 atm, the temperature being reduced slowly (42 h) to room temperature. The sample was quickly placed inside a He-filled dry box, without contact with the air, crushed to powder and encapsulated in a Pyrex tube. Finally, the glass tube was sealed off. The concentration was determined by pressure difference measurements with a Baratron manometer to the accuracy of ± 0.01 for the D/Y ratio.

The NMR measurements were performed with a Bruker MSL-300 pulse spectrometer at a frequency of 46.02 MHz using a Thor superconducting magnet. The ^{2}H NMR spectra were obtained by performing the Fourier transform of the ^{2}H free induction decay following a single pulse of 2 μs. The saturation-recovery sequence with a series of three saturation pulses of 10 μs separated by 0.5 ms was used to measure the spin-lattice relaxation time T_1. The temperature of the sample was controlled by flowing nitrogen gas and measured with a Cu–Constantan thermocouple.

COMPUTATIONAL DETAILS

The calculations are based on the density-functional theory[21,22] (DFT) and the local-density approximation and have been performed by the linearized augmented plane-wave (LAPW) method[23] in its full-potential version[24–27] (FLAPW) using an exchange-correlation potential by Hedin and Lundqvist.[28,29]

The parameters in the FLAPW calculation have been chosen as follows and are the same for both structures except where indicated explicitly. For the l expansion of the potential and the electron density inside the muffin-tin spheres terms up to $l=8$ were taken into account. In agreement with our previous calculations[18] the muffin-tin radii for Y and D were set to 1.4027 Å and 0.7062 Å, respectively. Plane waves for the wave functions in the interstitial region were included up to a length of 4.0 in units of $2\pi/a$, a choice that corresponds to ~ 1700 basis functions per unit cell (for six formula units of YD$_3$). In the self-consistency procedure for the valence states an irreducible set of 88 **k** points for the $P\bar{3}c1$ structure and 60 **k** points for the $P6_3cm$ structure have been used, corresponding to a $9\times9\times9$ Monkhorst and Pack[30] mesh. In order to describe the polarization of the higher-lying core states ("semicore states") of Y correctly, which is necessary to obtain accurate EFG's, the Y $4s$ and $4p$ states have been treated as band states in a second energy window for which irreducible sets of 19 and 15 **k** points were used for the $P\bar{3}c1$ and $P6_3cm$ structure, respectively, corresponding to a $5\times5\times5$ Monkhorst and Pack mesh in both cases. For the reciprocal-space integration the linear tetrahedron method[31,32] including the Blöchl correction[33] has been employed.

While in our recent paper,[18] where the Y EFG's have not been calculated, the Y $4s$ and $4p$ states were treated within the core approximation, we found it necessary for accurate EFG's to account for the band dispersion of these states. Furthermore, for maximum accuracy of the EFG's, the nonspherical terms of the matrix elements have been calculated for the full Hamiltonian, whereas in our previous study the *second variation* technique was used.

The EFG's have been calculated by taking the $l=2$ components of the Coulomb potential near the Y or D nuclei. The formalism by Herzig[17] and Blaha *et al.*[34] has also been employed to split the calculated EFG components into the contributions from the surrounding electrons within the respective muffin-tin sphere ("valence contribution") and the remainder that comes from outside this sphere ("lattice contribution"). This partitioning depends, to a small extent, on
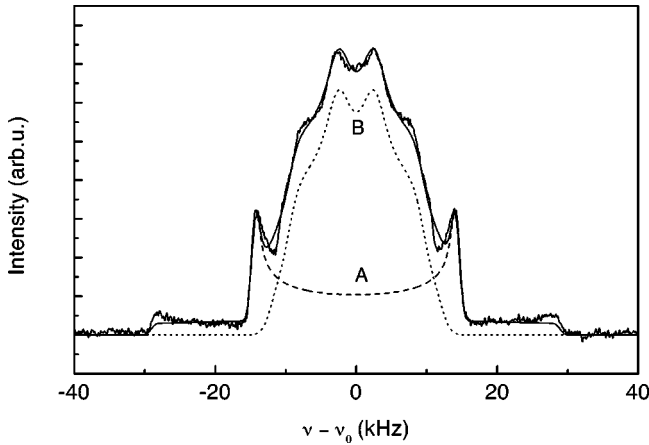
FIG. 1. Observed and synthesized (solid line) deuteron NMR spectra in YD$_{2.98}$ taken at $T = 180$ K. The simulated spectrum is a sum of the A and B components as described in the text.

the choice of the muffin-tin radii. The valence contribution can be split further into sd, pp, dd, pf, and ff contributions that provide useful information about the influence of particular l-like wave functions on the EFG's.[35]

RESULTS AND DISCUSSION

Among the spectra measured between 180 K and 380 K, those belonging to the temperature interval of 180–290 K show very little change. This suggests that deuteron motion such as atomic diffusion does not influence their shapes to a large extent. Thus, they reflect EFG's at the deuterium sites, specific for the given crystal structure at lower temperatures. A spectrum typical for the mentioned temperature range is shown in Fig. 1. It is obtained at the lowest temperature (180 K) used in our investigations. The spectrum can be considered as the superimposition of two components with different ν_q and η. For the deuterons, the first parameter is defined as

$$\nu_q = 3e^2qQ/2h, \tag{1}$$

where $eq = V_{zz}$ is the largest eigenvalue of the EFG tensor, Q is the deuteron quadrupole moment, and h is the Planck constant. The asymmetry parameter η is defined by

$$\eta = \frac{|V_{xx} - V_{yy}|}{|V_{zz}|}, \tag{2}$$

where V_{xx} and V_{yy} are the remaining two eigenvalues of the EFG tensor. The two components of the spectrum in Fig. 1 have the following parameters: $\nu_q = 58$ kHz, $\eta = 0$ for component A and $\nu_q = 24$ kHz, $\eta = 0.59$ for component B. Their integral intensities are 33.5% and 66.5% of the whole spectrum, for components A and B, respectively.

At this point let us mention the results of the NMR studies for YD$_3$ by Balbach et al.[19] Although they did not make the kind of simulation shown above, their 28 kHz doublet (referred to as cusp-to-cusp frequency width) fits the 29 kHz splitting well ($\nu_q/2$) for the A component. They, too, relate this feature of their spectrum, taken at 200 K, to octahedral sites. However, because of difficulties in their study to separate this part of the spectrum from the rest, 30–40% of the total intensity is a rather rough estimate of the expected 33%.

Now, in order to assign these lines we refer to the structural data available from neutron studies. Let us start with those proposed for the HoD$_3$-like structure of YD$_3$ (space group $P\bar{3}c1$, no. 165).[4] The two different types of the D atoms may be identified with the 12 tetrahedral and 6 octahedral D atoms (per 6 metal atoms) in the hexagonal close-packed structure. In the enlarged unit cell (HoD$_3$), the 12 distorted tetrahedral sites remain, which are all crystallographically equivalent. The 6 octahedral positions separate into 4 sites slightly above and below the metal-atom planes and 2 sites in the plane. Since the EFG is sensitive to the local symmetry, its tensor should be axially symmetric ($\eta = 0$) for the octahedral sites of both kinds as a consequence of the considered crystal structure. The ν_q parameters need not necessarily be the same but, as follows from the theoretical calculations (see below), they differ only slightly. In contrast to the octahedral sites, the tetrahedral site symmetry is lower than axial (there are three different distances to the four yttrium atoms in the HoD$_3$-like structure) and therefore $\eta \neq 0$ is expected. Based on the above considerations we may assign the A component as originating from the octahedral sites while the B component is due to the tetrahedral sites.

A similar analysis can be carried out for the crystal structure with the space group $P6_3cm$ (no. 185). In this case there are 6 octahedral sites ($4b$ and $2a$) for which the point symmetry requires axial symmetry of the EFG. The remaining 12 tetrahedral sites are divided into two groups ($6c$ each) with slightly different x, y, z parameters. Also in this case the EFG can have nonaxial symmetry. Therefore, if we assume the same values of the EFG for all tetrahedral sites and different values for all octahedral sites (which again are identical among each other), two components in the spectrum with a 2:1 intensity ratio are expected.

Now, in order to indicate which type of the crystal structure corresponds better to the NMR observation we present the theoretical EFG calculations performed for the present work. Table I summarizes these results. The structure models I and II refer to the HoD$_3$-like structure. The designation of the structure models and the corresponding parameters were taken from the paper by Udovic et al.[4] The structure models I and II are those that have only fully occupied deuterium sites, whereas the other structure models of Ref. 4 include partially occupied sites and have therefore not been considered in our study. The crystal structure information on the $P6_3cm$-type structure was obtained from Udovic;[36] the corresponding structure model is designated here as III. Since the structural parameters for model III became available to us only recently, results for this structure could not be provided in our previous paper,[18] where exclusively deuterium EFG calculations for structures I and II were presented. Numerical differences to the present results are essentially due to the different treatment of the yttrium inner-shell electrons.

For both types of structures the EFG calculations confirmed larger quadrupolar splitting ($\nu_q/2$) for the octahedral sites than for the tetrahedral sites, also in agreement with the

TABLE I. Comparison of calculated EFG's for the three model structures (I, II, III) with experimental results. The V_{zz} values are in units of 10^{20} V/m^2, the ν_q values in units of kHz, and lattice parameters in Å.

	Structure model		Site	V_{zz}	ν_q	η	Lattice parameter
I	Y:6f	$x=0.6665$		21.6		0.33	$a=6.3442$
	D(T):12g	$x=0.3542$	T	-2.2	22.9	0.78	$c=6.5997$
		$y=0.0311$					
		$z=0.0902$					
	D($m1$):2a		$O(m1)$	-6.0	62.6	0.0	
	D($m2$):4d	$z=0.1874$	$O(m2)$	-5.0	52.1	0.0	
II	Y:6f	$x=0.6637$		21.7		0.45	$a=6.3440$
	D(T):12g	$x=0.3521$	T	-2.2	22.9	0.78	$c=6.5997$
		$y=0.0321$					
		$z=0.0903$					
	D($m1$):2a		$O(m1)$	-5.7	59.4	0.0	
	D($m2$):4d	$z=0.1882$	$O(m2)$	-5.1	53.2	0.0	
III	Y:6c	$x=0.6717$		20.9		0.73	$a=6.3441$
		$z=0.25$					$c=6.5998$
	D(1):6c	$x=0.3054$	T	-2.3	23.5	0.65	
		$z=0.0898$					
	D(2):6c	$x=0.3601$	T	2.0	21.0	0.61	
		$z=0.4090$					
	D(3):2a	$z=0.3166$	O	-5.3	55.5	0.0	
	D(4):4b	$z=0.2073$	O	-5.2	54.3	0.0	
Expt.	D			2.3	24.0±1	0.59±0.05	
	D			5.6	58.0±1	0.0	

analysis of our spectra. Furthermore, the asymmetry parameter η is equal to zero for the octahedral positions as it also results from our decomposition for the A component. Although there are two different octahedral sites [D(3) and D(4)] in the $P6_3cm$-type structure with V_{zz} equal to -5.3×10^{20} V m^{-2} and -5.2×10^{20} V m^{-2}, respectively, they are indistinguishable in the spectra, because the finite lifetime of the transverse nuclear magnetization leads to a smoothing of the distribution function resulting from quadrupolar interaction alone. A similar argument applies to the D(1) and D(2) atoms belonging to the tetrahedral sites.

The η value for the tetrahedral sites (T) is not equal to zero for both types of structures. There is a substantial difference between the η values for the HoD$_3$- and $P6_3cm$-type structures. Such a difference easily manifests at the center of the spectrum, since a convex shape is expected for $\eta \sim 1$ and a concave one for $\eta \sim 0.5$ (Ref. 37). The experimental spectrum shows a concave shape at the center and its value of $\eta = 0.59$ obtained for the B component clearly favors the $P6_3cm$-type structure model when comparing to the calculated values, $\eta = 0.65$ and 0.61. Also the absolute values for V_{zz} (only these are available in the NMR experiment) as calculated for structure III agree very well with the experimental ones.

Analyzing the contributions to the EFG from the valence electrons inside and the charge distribution outside the respective muffin-tin sphere, we observe a quite distinct behav-

ior for Y and D. The EFG's for yttrium are defined almost completely by its valence contribution (99%). The EFG for deuterium, on the other hand, is predominantly determined by its lattice contribution with a 3–4 times larger absolute value than that for the valence part. For Y the pp component dominates the ll' decomposition whereby a smaller dd component is also found.

As the temperature is increased above 290 K, changes in the spectra appear. In the beginning (300 K), the convex top at the center flattens and a central resonance line of very small intensity arises. A further temperature increase generates two doublets with $\nu_q = 33$ and 16.5 kHz, in addition to that with $\nu_q = 58$ kHz, already present at 180 K, and an intensity increase of the central component as is illustrated in Fig. 2. The easiest interpretation of these doublets would be to assume a motion of tetrahedral deuterium taking place, since the 58 kHz octahedral D doublet is hardly affected by the temperature changes. The character of this motion must be such that the two different deuterium sites, both with a Wyckoff symbol of 6c, remain distinct (we consider the $P6_3cm$-type structure from now on—see Table I). In the other case, a single resonance line would be expected where fast D atom interchanges between the different 6c sites were to occur. Therefore correlated hopping of the deuterons between nearby sites in ab planes shall now be considered. This movement will change the shape of the spectrum depending on the orientation between the principal axis of the
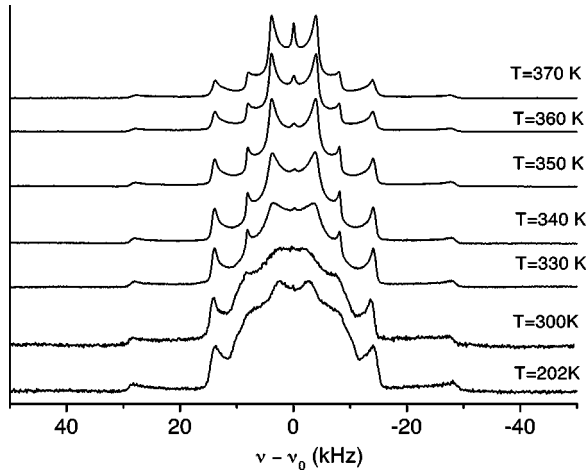
FIG. 2. Temperature evolution of the deuteron NMR powder spectra in YD$_{2.98}$. Incipient superimposition of the three quadrupolar doublets is seen at $T=300$ K. The outermost, intermediate, and innermost doublets correspond to $\nu_q=58$, 33, and 16.5 kHz, respectively.

EFG tensor and the axis about which the hopping takes place, which is a threefold symmetry axis in the present example. We have simulated the spectrum assuming that the principal axes (i.e., the axes for the V_{zz} components) of the EFG tensors for the three deuterons at the corners of equilateral triangles lie in the ab plane and are aligned towards the centers of the dashed triangles shown in Fig. 3. The ori-
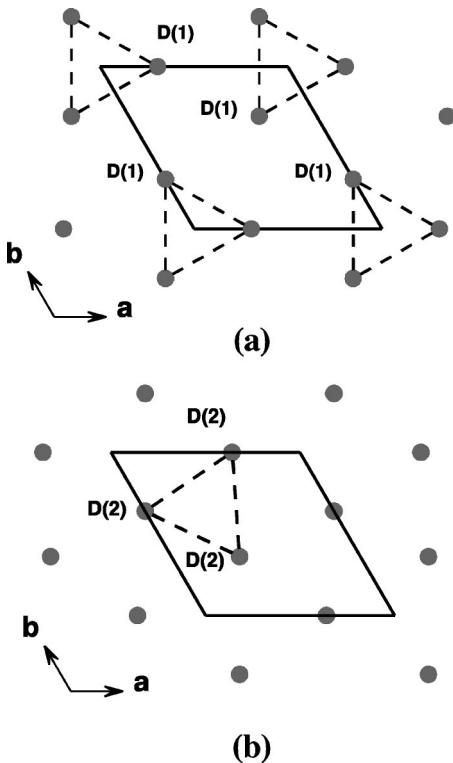
FIG. 3. Schematic drawings in the (001) plane of (a) the D(1) triads at $z=0.0898$ and (b) a D(2) triad at $z=-0.0910$. For the D(1) atoms the correlated hopping of deuterons along each side of a triangle would form a doublet with $\nu_q=17.3$ kHz.
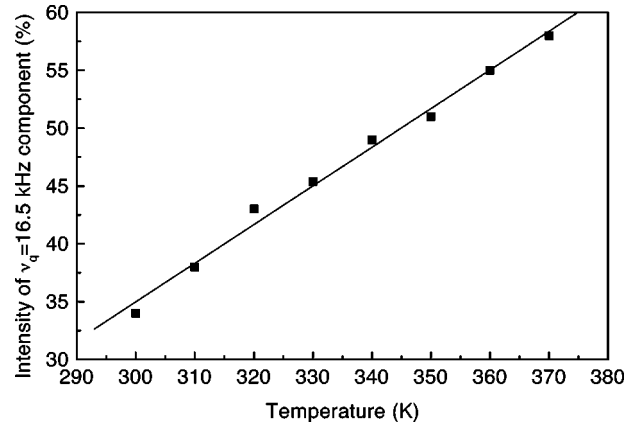

FIG. 4. Intensity of the doublet with $\nu_q=16.5$ kHz versus temperature. The line is a guide to the eye.

entation of the other two axes (for V_{xx} and V_{yy}), which are perpendicular to that for V_{zz}, has no influence on the simulated spectrum. The hopping occurs as a correlated cyclic exchange of the deuterium atoms at the corners of these dashed triangles. Values of ν_q equal to 24 kHz and $\eta=0.59$ are used and it is assumed that the motion rate is much greater than ν_q for these sites. The resulting simulated spectrum yields a quadrupolar doublet with $\nu_q=17.3$ kHz, close to one of the doublets observed at elevated temperatures (above 290 K). The other tetrahedral site subset may have a larger ν_q, because of the absence of fast deuteron jumps at lower temperatures. While at these lower temperatures the η value for D(2) appears to be the same as that for D(1) ($\eta=0.59$), a value of $\eta=0$ is observed (Fig. 2) at higher temperatures. This could either be due to a small displacement of the deuteron position inside the yttrium tetrahedron or due to fast "rattling" around its symmetry center. Both effects could be stimulated by deuteron hopping in the D(1) tetrahedral site subset. Figure 4 shows the integral intensity of the component with $\nu_q=16.5$ kHz versus temperature. The intensity grows with temperature at the expense of the doublet with $\nu_q=33$ kHz. This can be interpreted by an increasing number of hopping D(2) atoms with increasing temperature. The intensity of the outermost doublet (at 58 kHz) exhibits only a weak temperature dependence. In addition to the three doublets, a sharp central line begins to grow with increasing temperature and reaches about 3% of the total intensity at $T=370$ K. It is likely due to diffusion of the deuterons over many sites in the three-dimensional (3D) crystal space.

Let us add that a consequence of this model for the deuteron motion in the plane would be a "layer" structure, i.e., an increased anisotropy of the YD$_3$ configuration, contrary to the situation where there is deuteron hopping in 3D space. In fact, two-dimensional (2D) weak localization or Kondo scattering was suggested to explain the logarithmic divergence of the electric resistivity in YH$_{3-\delta}$ (Ref. 38).

In addition to the ^{2}H NMR spectra, the spin-lattice relaxation rates, $1/T_1$, were also measured. These results are close to those reported by Balbach et al.[19] There is a sharp rise of $1/T_1$ near 290 K typical for thermally activated motion of the D atoms. The activation energy is deduced to be E_a

=0.50(2) eV, well within the range of 0.45–0.55 eV estimated from their experiments.

CONCLUSIONS

The calculations of the electric field gradients for the $P\bar{3}c1$ and $P6_3cm$ structures and their comparison with the experimental values obtained from ^{2}H NMR experiments clearly favor the latter structure. The best fit of the experimental spectra has been obtained with the tetrahedral asymmetry parameter $\eta=0.59$. The closest agreement with the η value mentioned above was obtained from first-principles calculations for the $P6_3cm$ structure, yielding the η values 0.65 and 0.61 for the respective tetrahedral D sites. At low temperatures, the decomposition of the spectra into two constituents with an intensity ratio of $\frac{2}{3}:\frac{1}{3}$ is in accord with the proposed structure type, which has two inequivalent groups of deuterons, namely D atoms at tetrahedral and octahedral sites in the above proportion. Although the tetrahedral sites in the space group $P6_3cm$ split into two subsets of $6c$ Wyckoff symmetry each and similarly the octahedral sites into $4b$ and $2a$, their EFG values are not different enough to be resolved in the present experiment.

At higher temperatures (above 300 K) the motion-driven fluctuations in the quadrupole interaction cause remarkable changes in the spectra. While the octahedral site component remains unchanged, the second is split into two doublets with a 1:1 intensity ratio at the beginning. The distance between the cusps of the innermost doublet, 8.25 kHz, is such that it can correspond to deuteron jumps to nearby sites in the ab plane. When the temperature is raised to 370 K, the intensity of this component grows at the expense of the second "tetrahedral" one ($\nu_q=33$ kHz). This would indicate that gradually all tetrahedral D atoms start hopping. In addition, a narrow central resonance line is observed whose intensity increases with temperature, taking up a few percent of total intensity at the highest temperature used. The atomic motion of deuterons amidst many deuteron positions is responsible for its presence. The temperature dependence of the spin-lattice relaxation times confirms the thermal activation energy for deuteron motion earlier reported by Balbach et al.[19]

[1] J.N. Huiberts, R. Griessen, J.H. Rector, R.J. Wijngaarden, J.P. Dekker, D.G. de Groot, and N.J. Koeman, Nature (London) **380**, 231 (1996).
[2] N.F. Miron, V.I. Shcherbak, V.N. Bykov, and V.A. Levdik, Kristallografiya **17**, 404 (1972) [Sov. Phys. Crystallogr. **17**, 342 (1972)].
[3] A. Pebler and W.E. Wallace, J. Phys. Chem. **66**, 148 (1962).
[4] T.J. Udovic, Q. Huang, and J.J. Rush, J. Phys. Chem. Solids **57**, 423 (1996).
[5] T.J. Udovic, Q. Huang, and J.J. Rush, in Hydrogen in Semiconductors and Metals, edited by N. N. Nickel, W. B. Jackson, R. C. Bowman, and R. G. Leisure, MRS Symposia Proceedings No. 513 (Materials Research Society, Pittsburgh, 1998), p. 197.
[6] T.J. Udovic, Q. Huang, R.W. Erwin, B. Hjörvarsson, and R.C.C. Ward, Phys. Rev. B **61**, 12 701 (2000).
[7] H. Kierey, M. Rode, A. Jacob, A. Borgschulte, and J. Schoenes, Phys. Rev. B **63**, 134109 (2001).
[8] Y. Wang and M.Y. Chou, Phys. Rev. Lett. **71**, 1226 (1993).
[9] Y. Wang and M.Y. Chou, Phys. Rev. B **51**, 7500 (1995).
[10] J.P. Dekker, J. van Eck, A. Lodder, and J.N. Huiberts, J. Phys.: Condens. Matter **5**, 4805 (1993).
[11] P.J. Kelly, J.P. Dekker, and R. Stumpf, Phys. Rev. Lett. **78**, 1315 (1997).
[12] R. Ahuja, B. Johansson, J.M. Wills, and O. Eriksson, Appl. Phys. Lett. **71**, 3498 (1997).
[13] R. Eder, H.F. Pen, and G.A. Sawatzky, Phys. Rev. B **56**, 10 115 (1997).
[14] T. Miyake, F. Aryasetiawan, H. Kino, and K. Terakura, Phys. Rev. B **61**, 16 491 (2000).
[15] P. van Gelderen, P.A. Bobbert, P.J. Kelly, and G. Brocks, Phys. Rev. Lett. **85**, 2989 (2000).
[16] P. van Gelderen, P.J. Kelly, and G. Brocks, Phys. Rev. B **63**, 100301 (2001).
[17] P. Herzig, Theor. Chim. Acta **67**, 323 (1985).
[18] P. Herzig, W. Wolf, and O.J. Żogal, Phys. Rev. B **62**, 7098 (2000).
[19] J.J. Balbach, M.S. Conradi, M.M. Hoffmann, T.J. Udovic, and N.L. Adolphi, Phys. Rev. B **58**, 14 823 (1998).
[20] M. Forker, U. Hütten, and M. Lieder, Phys. Rev. B **49**, 8556 (1994).
[21] P. Hohenberg and W. Kohn, Phys. Rev. **136**, B864 (1964).
[22] W. Kohn and L.J. Sham, Phys. Rev. **140**, A1133 (1965).
[23] O.K. Andersen, Phys. Rev. B **12**, 3060 (1975).
[24] D.D. Koelling and G.O. Arbman, J. Phys. F **5**, 2041 (1975).
[25] E. Wimmer, H. Krakauer, M. Weinert, and A.J. Freeman, Phys. Rev. B **24**, 864 (1981).
[26] H.J.F. Jansen and A.J. Freeman, Phys. Rev. B **30**, 561 (1984).
[27] B.I. Min, T. Oguchi, H.J.F. Jansen, and A.J. Freeman, J. Magn. Magn. Mater. **54-57**, 1091 (1986).
[28] L. Hedin and B.I. Lundqvist, J. Phys. C: Solid State Phys. **4**, 2064 (1971).
[29] L. Hedin and S. Lundqvist, J. Phys. (Paris), Colloq. **33**, C3-73 (1972).
[30] H.J. Monkhorst and J.D. Pack, Phys. Rev. B **13**, 5188 (1976).
[31] O. Jepsen and O.K. Andersen, Solid State Commun. **9**, 1763 (1971).

[32] G. Lehmann and M. Taut, Phys. Status Solidi B **54**, 469 (1972).

[33] P.E. Blöchl, O. Jepsen, and O.K. Andersen, Phys. Rev. B **49**, 16 223 (1994).

[34] P. Blaha, K. Schwarz, and P. Herzig, Phys. Rev. Lett. **54**, 1192 (1985).

[35] P. Blaha, K. Schwarz, and P.H. Dederichs, Phys. Rev. B **37**, 2792 (1988).

[36] T. J. Udovic (private communication).

[37] J. L. Dye and A. S. Ellaboudy, in *Modern NMR Techniques and Their Application in Chemistry*, edited by A. I. Popov and K. Hallenga (Marcel Dekker, New York, 1991), p. 244.

[38] J.N. Huiberts, R. Griessen, R.J. Wijngaarden, M. Kremers, and C. Van Haesendonck, Phys. Rev. Lett. **79**, 3724 (1997).